Published in final edited form as:
Biomaterials. 2013 September ; 34(28): 6938–6948. doi:10.1016/j.biomaterials.2013.05.047.

Adenoviral vector tethering to metal surfaces via hydrolysable cross-linkers for the modulation of vector release and transduction

Ilia Fishbein[1,2], **Scott P. Forbes**[1], **Michael Chorny**[1,2], **Jeanne M. Connolly**[1], **Richard F. Adamo**[1], **Ricardo Corrales**[1], **Ivan S. Alferiev**[1,2], and **Robert J. Levy**[1,2]

[1]Division of Cardiology, The Children's Hospital of Philadelphia, Abramson Research Center, Philadelphia, PA

[2]Department of Pediatrics, Perelman School of Medicine of the University of Pennsylvania, Philadelphia, PA

Abstract

The use of arterial stents and other medical implants as a delivery platform for surface immobilized gene vectors allows for safe and efficient localized expression of therapeutic transgenes. In this study we investigate the use of hydrolysable cross-linkers with distinct kinetics of hydrolysis for delivery of gene vectors from polyallylamine bisphosphonate-modified metal surfaces. Three cross-linkers with the estimated $t_{1/2}$ of ester bonds hydrolysis of 5, 12 and 50 days demonstrated a cumulative 20%, 39% and 45% vector release, respectively, after 30 days exposure to physiological buffer at 37°C. Transgene expression in endothelial and smooth muscles cells transduced with substrate immobilized adenovirus resulted in significantly different expression profiles for each individual cross-linker. Furthermore, immobilization of adenoviral vectors effectively extended their transduction effectiveness beyond the initial phase of release. Transgene expression driven by adenovirus-tethered stents in rat carotid arteries demonstrated that a faster rate of cross-linker hydrolysis resulted in higher expression levels at day 1, which declined by day 8 after stent implantation, while inversely, slower hydrolysis was associated with increased arterial expression at day 8 in comparison with day 1. In conclusion, adjustable release of transduction-competent adenoviral vectors from metallic surfaces can be achieved, both *in vitro* and *in vivo*, through surface immobilization of adenoviral vectors using hydrolysable cross-linkers with structure-specific release kinetics.

INTRODUCTION

Gene therapy holds promise for providing unique remedies to treat human diseases. However, its clinical implementation is hampered by several formidable obstacles, such as insufficient levels and duration of transgene expression at the target site, off-target inoculation of healthy tissues and vector-triggered immune and inflammatory responses [1]. Along with increased sophistication in vector engineering [2], advanced methods of vector delivery to the site of action have recently emerged as potential solutions for overcoming the

Corresponding author's address: Ilia Fishbein, The Children's Hospital of Philadelphia, Abramson Research Center, 3615 Civic Center Blvd, PA 19104, USA Telephone number: (215)590-8740 Fax number: (215)-590-5454 fishbein@email.chop.edu.

limitations of experimental and clinical gene therapy systems [3]. One of the main directions explored in an attempt to resolve the inherent challenges of gene therapy is localized delivery of gene vectors [3, 4]. Spatial restriction of vector localization and ensuing transgene expression to the disease site is highly desirable in focal pathological processes, such as solid tumors [5], fibrotic reactions [6] and cardiovascular diseases [3, 7]. The latter group has an added advantage of direct accessibility via well-developed vascular catheterization techniques [3, 8]. Furthermore, interfacing gene therapy with medical implants presents an opportunity for increasing the effectiveness of localized gene transfer, limiting side effects related to off-site transduction and promoting healing of tissue surrounding the implanted device [9]. To this end, immobilization of gene vectors on the surface of medical implants results in a highly controllable transgene expression in the tissues directly adjacent to the implant, achieved via a process termed “reverse transfection” [10] or “substrate mediated gene transfer” [11, 12]. Moreover, vector immobilization allows for modulation of vector release rates, and both the extent and duration of transgene expression [13].

Endovascular stents [14] deployed in the coronary and peripheral arteries to relieve atherosclerotic occlusions are by far the most often used implants in medical practice [15]. The effectiveness of stents as a frontline approach for treating patients with symptomatic atherosclerosis is marred by a 5-15% rate of in-stent restenosis (a secondary re-obstruction of treated arteries due to unresolved inflammation and activation of smooth muscle cells in arterial wall) [16]. For more than 20 years restenosis has represented a putative target for gene therapy [17, 18]. A number of experimental strategies have been investigated to make use of stents as delivery platforms for both non-viral [19-25] and viral [26-32] gene therapy formulations for the prevention of restenosis.

Our previous work has explored reversible immobilization of adenoviral vectors on polyallylamine bisphosphonate-modified uncoated stainless steel surfaces of endovascular stents using either vector-specific affinity binding-protein adaptors [26] or synthetic hydrolysable cross-linkers (HC) [27] to tether vectors to the substrate. Two water-soluble polyallylamine bisphosphonate compounds utilized in our past studies (lacking (PAB) [26] , and comprising (PABT) [27] installed latent thiol groups) were shown to create an ultra-thin (< 5 nm) monolayer arrangement on the surface of steel and other alloys due to the formation of strong coordination bonds between the bisphosphonic groups and the metals and metal oxides of the steel surfaces. This “coatless” method of vector immobilization distinguishes our approach from other studies employing multi-micron polymer coatings of the stent struts to incorporate gene vectors in the bulk of the polymer. Both, our affinity binding [26] and HC tethering [27] Ad immobilization strategies have demonstrated effective local transduction of vascular tissue and inhibition of restenosis in stented arterial segments using stents configured with Ad vectors encoding inducible nitric oxide synthase (Ad-iNOS). Since the immobilization scheme realized using cleavable (hydrolysable) cross-linkers [27] allowed for better control of vector loading and release, it was chosen for further development of stent-based gene delivery. Our present work focused on a family of chemically related cross-linkers with dissimilar kinetics of hydrolysis. Here we report on studies that investigated vector release kinetics and subsequent transgene expression *in vitro* and *in vivo* as a function of the hydrolysis rate of cross-linkers used for vector immobilization on steel surfaces.

MATERIALS AND METHODS

Adenoviral vectors

Replication defective type 5 (E1, E3 deleted) Ad were used in these studies. All vectors were constructed with the human cytomegalovirus promoter. Both Ad expressing enhanced

green fluorescent protein (GFP) and Ad expressing firefly luciferase (Luc) were obtained from the Gene Vector Core of the University of Pennsylvania (Philadelphia, PA).

Chemicals

The chemicals used for Ad conjugation to steel surface, were either synthesized in-house (PABT, PEI_{PDT}, HC) or were purchased from Thermo Scientific (Rockford, IL) (TCEP - [Tris-(2-carboxyethyl) phosphine], DTT – dithiothreitol, and non-hydrolysable cross-linker, sulfo-LC-SPDP [sulfosuccinimidyl 6-(3′-[2-pyridyldithio]-propionamido)hexanoate]). Remaining chemicals and biologicals were from Sigma-Aldrich (St. Louis, MO) unless indicated otherwise in the text. The synthesis and characterization of PABT and PEI_{PDT} were previously reported [27].

Synthesis and characterization of hydrolysable cross-linkers (HC)

Three HC with different kinetics of ester bond hydrolysis in the linker backbone (rapidly, intermediately and slowly hydrolysable cross-linkers, referred to as RHC, IHC and SHC respectively) were synthesized and characterized in our laboratory as follows.

To synthesize the RHC ($t_{1/2}$=5 d), 2-(2-pyridyldithio)-ethanol was esterified with N-succinimidyl ester of Boc-glycine. The protective group was removed, the resulting amine was reacted with adipic anhydride, and the corresponding amido-acid was transformed into its N-sulfosuccinimidyl ester.

For the synthesis of IHC ($t_{1/2}$=12 d) 2-(2-pyridyldithio)-ethanol was reacted with succinic anhydride. The resulting hemi-ester was activated via N-succinimidyl-derivatization and coupled with 6-aminocaproic acid, with the final formation of N-sulfosuccinimidyl ester.

To prepare SHC ($t_{1/2}$=50 d), SPDP was reacted with 3-aminopropanol. The resulting alcohol containing a 2-pyridyldithio group was reacted with adipic anhydride, and finally, N-sulfosuccinimidyl ester was formed from the remaining carboxylic group.

Design of the ester groups in the cross-linkers was selected based on the hydrolysis kinetics of model esters as follows: 1) N-acetylglycine ethyl ester as a model of RHS, 2) ethyl N-butylsuccinamate as a model of IHC and 3) ethyl acetate, modeling SHC. Hydrolysis rates of the model esters were measured using ^{1}H NMR monitoring in phosphate buffer at pH = 7 and 22°C, resulting in $t_{1/2}$ 27 d, 63 d and >200 d for the models of RHC, IHC and SHC correspondingly. These values were corrected for the effects of temperature resulting in the estimated $t_{1/2}$ of 5, 12 and 50 days for ester hydrolysis of the model molecules, respectively.

Immobilization of adenoviral vectors on stainless steel surfaces

316 grade stainless steel mesh disks (Electron Microscopy Sciences, Hatfield, PA) or 304 grade stainless steel stents (Laserage, Waukegan, IL) were cleansed with isopropanol/1.5 N nitric acid, prior to the incubation in 1.5% PABT/DDW (pH 4.5) at 72°C for 4 hours with shaking. The samples were washed with DDW, treated with 20 mg/ml TCEP in 0.1M acetic buffer at 28°C for 20 min with shaking, washed again with degassed DDW and reacted in an argon atmosphere with 2% PEI_{PDT}/DDW (pH 4.5) at 28°C for 2 hours with shaking, followed by the conversion of PTD groups to thiols upon exposure to DTT/DDW (20 mg/ml) at 28°C for 10 minutes.

In parallel with the steel surface modification, 2×10^{11} particles of Ad were diluted with 300 μl of carbonate/bicarbonate buffer (pH 9.3) and exposed to either RHC, IHC, SHC or NHC (30-500 μM final concentrations) for at 28°C for 1 hour. The modified Ad was then gel-filtrated via Sepharose 6B (Sigma, St. Louis, MO) into degassed PBS/10 mM EDTA with a

typical yield of 75-85%. The tethering of thiol-reactive Ad vectors to thiolated metal surfaces was achieved by incubations at 28°C for 2 h in an argon atmosphere in the presence of 1% maleimide-capped BSA to minimize non-specific binding of the vector.

To facilitate detection of immobilized vector in the release experiments, Ad vectors were co-modified by reacting them with both HC and the amine-reactive fluorescent dye, Cy3-NHS_2 (GE Healthcare, Piscataway, NJ). Briefly, Ad virus prep (2×10^{12} particles) was first modified with Cy3-NHS_2 followed by purification using gel-filtration via Sepharose 6B and concentration with centrifugal filter devices (Centriprep YM-30; EMD Millipore, Billerica, MA) with an overall yield of 55-60% as estimated by light absorbance at 260/280 nm. The average number of fluorophore molecules attached to a virus capsid was 746 (i.e. less than 5% of all amine groups exposed on the surface of Ad particle [33]). Cy3-labeled Ad was then further reacted with RHC, IHC, SHC and NHC at amine groups that were not consumed during the labeling step. The further purification and conjugation of Cy3-labeled Ad was carried out as indicated above for non-labeled vectors. The number of fluorescently labeled Ad particles attached to the meshes was determined fluorimetrically by the depletion of a fluorescent suspension of viral particles using the experimentally resolved ratio between fluorescent and spectrophotometric scales. Additionally, the Ad immobilization yield with different cross-linkers was determined by qPCR. Ad-GFP was attached to the meshes using RHC, IHC, SHC or NHC tethering. Adenoviral DNA was eluted from the surface of meshes using a QIAamp mini kit (Qiagen, Germantown, MD) per manufacturer instructions. The DNA was amplified in a Sybr Green reaction using GFP-specific primers (forward: 5′ CTC CTC GCC CTT GCT CAC 3′, reverse: 5′ CAG TGG ATG TTG CCT TTA CTT CTA G 3′) along with DNA extracted in a similar way from a known amount of Ad-GFP.

Ad release experiments

To determine the release rate of Ad vectors immobilized on steel surfaces via HC/PABT-PEI_{PDT} chemical interactions, meshes formulated with 2×10^9 Cy3-labeled Ad particles per mesh were individually incubated in release buffer (0.1% BSA/0.1% TWEEN-20/PBS) at 37°C with shaking (50 rpm). The release of Cy3-labeled Ad from the mesh surfaces was examined by fluorescence microscopy and fluorometry using standardized microscope, CCD camera and fluorometry plate reader setting for 30 days. Prior to each measurement the release buffer was withdrawn and replaced with fresh release buffer.

Cell culture experiments

Meshes derivatized with approximately 2×10^9 Ad-GFP particles (immobilization density of $3\times10^{10}/cm^2$) were individually placed on top of confluent BAEC or A10 cells (both from ATCC, Gaithersburg, MD) in the wells of 96-well plates. Transduction kinetics, assessed by GFP expression from cells treated with virus tethered meshes, was studied by fluorescence microscopy and well-scan fluorometry. The settings of the microscope, CCD camera software and fluorometer were kept constant for the duration of the experiment.

In a subset of cell culture experiments, designed to determine transduction competence of Ad vectors released from the meshes at the deferred time intervals after commencement of release, BAEC were removed from the wells 2 days after the mesh placement by trypsinization, followed by extensive *in situ* washing of the partially depleted meshes to remove transduced cells. After the completeness of GFP-positive cell elimination was confirmed by fluorescence microscopy and fluorometry, new non-transduced BAEC were re-plated over the partially released meshes. New transduction events caused by the virus particles subsequently released from the mesh carrier after the 2 day time point were then assessed by fluorescence microscopy and fluorometry.

Alternatively, a set of Ad-GFP-tethered meshes was placed on top of confluent BAEC not immediately upon formulation, but after 72 hours incubation in full DMEM with 10% FBS at 37°C with mild shaking. The transgene expression in this experiment was assessed by fluorescence microscopy and fluorometry as above.

Animal experiments

Custom-designed multi-link stainless steel (304 grade) stents were formulated with ~ 1.3×10^{10} Ad-Luc particles appended via RHC, IHC, SHC and NHC to the polyallylamine bisphosphonate-modified steel surface. Carotid stent angioplasties were carried out in 420-450 g male Sprague-Dawley rats. After performing carotid balloon denudation with 3 passages of a 2F Fogarty catheter (Edwards LifeSciences, Irvine, CA) the stents were deployed with PTA catheters (1.5 mm nominal diameter; NuMed, Hopkinton, NY) at 16 atm in the mid-segments of the left common carotid arteries as described in our previous publications [26, 27, 34, 35]. To compare *in vivo* transduction effectiveness and durability of vascular transgene expression with stent-tethered and non-immobilized vectors, an additional group of BMS-stented animals was intralumenally delivered with 1.3×10^{10} free Ad-Luc particles for 20 min. At days 1 and 8 after stent deployment, all animals underwent bioluminescent imaging (IVIS Spectrum, PerkinElmer, Waltham, MA) immediately after intravenous administration of 50 mg luciferin [27, 35].

Animal studies were approved by the Institutional Animal Care and Use Committee and conducted in accordance with principles and procedures outlined in the NIH Guide for the Care and Use of Animals.

Data analysis

Values expressed as means ± SE. Analysis of variance with a post-hoc Tukey test was employed to analyze the differences between the corresponding points in the release and transduction curves. Values of $P< 0.05$ were considered statistically significant.

RESULTS

Release of Ad vectors tethered to stainless steel surface via HC with different kinetics of hydrolysis

In order to study the effects of HC chemical structure on the release rate of Ad vectors, we utilized Ad vectors covalently modified with a fluorescent dye, Cy3 [36]. Since Cy3 labeling utilizes the same chemical reaction as HC modification [36], no more than 5% of the primary amines of the Ad capsid were consumed during fluorescent labeling (data not shown), thus preventing potential interference of Cy3 labeling with subsequent tethering of Ad vectors. Following completion of Cy3 labeling, the remaining amine functionalities on the virus surface were further modified with HC to render reactivity with the thiols groups introduced onto the stainless steel surface by sequential PABT coordination, thiol deprotection, PEI_{PDT} modification and PDT reduction ([27] and Fig. 1a;). Three HC with different kinetics of ester bond hydrolysis in the linker backbone, RHC, IHC and SHC, Fig. 1b), as well as a parent non-hydrolysable cross-linker compound, commercially available sulfo-LC-SPDP, designated as NHC (Fig. 1b), were used at a final concentration of 0.5 mM for vector modification. Additionally, a sample of Cy3-labeled Ad vector was modified with RHC at a 0.1 mM concentration. Following the attachment of approximately 2×10^{9} Cy3-labeled vectors to the surface of model stainless steel meshes, samples formulated using the different cross-linkers were individually placed into the wells of a 96-well plate in release buffer. Fluorescence microscopy images of mesh surface and fluorometry data sets generated immediately upon release commencement and at multiple time points in the

course of vector release were used for determining kinetics of Ad detachment from the metal substrate.

The relative intensities of surface-associated fluorescence signal decreased over the 30-day time course of this experiment (Fig. 2a). Vector release rates for NHC and SHC were virtually identical, suggesting a lack of hydrolysis-mediated vector release for SHC mediated vector tethering (Fig. 2a) in the time frame of this experiment. Therefore, the apparent release of 20% of the initial virus load with both NHC and SHC observed by day 9 and remaining invariable through day 30, likely represents loss of the vector physically adsorbed rather than chemically coupled onto the thiol-engrafted metal surface. Ad vectors attached through IHC and RHC linkages demonstrated significantly faster ($p<0.001$) detachment from the surface, resulting in respectively 39% and 45% release of the vector by day 30 (Fig. 2a). Finally, Ad vectors immobilized using a lower concentration of cross-linker (0.1 mM RHC, designated as RHC-L) resulted in a statistically faster ($p<0.05$) release rate as compared to vectors formulated according to the standard HC modification (0.5 mM RHC) protocol (Fig. 2a). The latter finding supports the mechanism according to which in addition to the chemical nature of the HC, the number of tethers between capsid and metal substrate plays an important role in determining the actual release rate of the vector, since all tethers that contain the vector near the metal surface must be hydrolyzed to allow virus release.

Fluorescence microscopy data used to corroborate the fluorometry-based quantitative release analysis (Fig. 2b), demonstrate a faster and more profound decrease of surface-associated fluorescence with mesh samples formulated using IHC-, RHC- and RHC-L-tethered vectors in comparison with their NHC- and SHC-tethered counterparts (Fig. 2b).

Transduction of SMC and endothelial cells with mesh-immobilized Ad-GFP tethered to steel surface using HC with different kinetics of hydrolysis

To test whether kinetics and overall transduction efficiency of substrate-immobilized Ad vectors can be modulated with the use of HC exhibiting different rates of the ester bond hydrolysis, we prepared mesh disks appended with equal amounts of Ad-GFP ($\sim 2\times10^9$ viral particles) using either NHC, SHC, IHC or RHC. Quantification of Ad particle immobilization on stainless steel meshes was based on 1) fluorimetrically estimated drop of Cy3Ad titer in the formulations of HC-modified Ad vectors exposed to the activated mesh samples in comparison with the same vector formulations incubated without the meshes, and 2) direct PCR-based enumeration of GFP gene copies associated with the individual meshes. Generally the PCR based estimation (Fig. 3) exceeded vector attachment as determined by fluorimetry by 180-280%, which is a satisfactory correspondence given vastly different assay methodologies and known caveats of quantitative PCR [37].

The mesh structure and material (stainless steel) were chosen to model vector immobilization onto and release from stent struts. The meshes were individually placed into the wells of a 96-well plate, and the ensuing GFP expression in transduced endothelial and SMC was studied over time by fluorescence microscopy and fluorometry.

Transgene expression in rat aortic smooth muscle cells (A10 cell line) brought about by Ad-GFP immobilized via SHC, IHC and RHC peaked at day 4 after mesh placement onto a monolayer of cells in culture (Fig. 4a and b). All types of HC provided significant spatial specificity of gene transfer with >95% of GFP-positive cells located under the mesh or within 500 microns from the mesh edge (Fig. 4a). The relative intensity of maximal GFP expression achieved with RHC-mediated tethering was more than 5-fold higher than one observed with SHC-mediated vector binding, while IHC-immobilized vectors resulted in peak levels of transgene expression intermediate between the SHC and RHC vector

immobilization values (Fig. 4a and b). The vectors appended via NHC (sulfo-LC-SPDP) resulted in minimal GFP expression at all time points (Fig. 4a and b), reflecting the lack of active release of transduction-competent viral particles.

In bovine aortic endothelial cells (BAEC) transduction brought about by mesh-immobilized Ad-GFP similarly peaked at 4 days post mesh placement (Fig. 4c and d), although the respective GFP expression levels were 2.5-fold higher in BAEC than in rat SMC (compare Fig. 4b and d). The relative fluorescence intensity values at peak transduction were 8-fold and 1.8-fold higher in wells treated with RHC tethered meshes, as compared to SHC and IHC tethered counterparts, respectively, essentially reproducing the transduction pattern observed in SMC. Although scattered GFP positive cells were present in wells treated with meshes formulated with NHC-immobilized Ad-GFP, the peak expression levels achieved with the vector linked to steel substrate using the non-cleavable cross-linker were significantly ($p<0.001$) lower than with any of the HC (Fig. 4b and d). It is important to note that after reaching a peak transgene expression at day 4, GFP expression produced by the RHC-containing mesh disks dropped steeply by days 7 and 9, while the GFP expression brought about by the IHC-containing meshes remained relatively stable, resulting in a crossover of the cell transduction curves at day 6 (Fig. 4d). This transgene expression pattern is compatible with the paradigm of more sustained release of gene vectors appended via the IHC tether in comparison with a shorter time course of the RHC hydrolysis-mediated Ad release and transduction.

To rule out the possibility that the vastly different transduction efficiencies of Ad vectors appended to the surface of mesh substrates via the three HC and their non-hydrolysable analog, sulfo-LC-SPDP, result from the varying extent of virus inactivation upon modification with different cross-linkers, we reacted identical Ad-GFP aliquots with 4 cross-linkers and used the modified non-immobilized Ad vectors for BAEC transduction. Under experimental conditions corresponding to those used for the mesh-tethered Ad-GFP transduction study, vector capsid modification with all 4 cross-linker molecules resulted in a significant ($p<0.001$) 100-150-fold drop of GFP expression in comparison with non-modified Ad-GFP (Fig. 4 e). However, no significant differences in vector transduction competences were observed among the vectors reacted with the 4 different cross-linkers (Fig. 4 e).

Transduction competence of Ad vectors released from mesh substrates at delayed time points

Two distinct experimental approaches were used to attest that Ad particles released from the mesh substrate at deferred time points after initiation of HC hydrolysis remained capable of effective transduction of underlying cells.

First, meshes configured with Ad-GFP vectors immobilized via NHC, SHC, IHC and RHC were used to transduce freshly confluent BAEC. After assessing the ongoing GFP expression at day 2 by fluorescence microscopy and fluorometry (Fig. 5a and b), the cells were trypsinized and removed from the wells without disturbing the virus-bearing meshes. Fresh non-transduced BAEC were then seeded into the wells, on top of the partially depleted meshes. The completeness of removal of the first-round BAEC was verified by fluorescent microscopy and fluorometry. The transduction of the second-round BAEC was then examined over time (Fig. 5a and b) demonstrating a 1.4-fold, 4-fold and 5.7-fold increase of the GFP specific signal between days 2.5 and 4 in the wells with re-plated cells, transduced with the partially depleted meshes configured using SHC, IHC and RHC for vector tethering, respectively. Since the only source of any transgene expression in the second-round (re-plated) BAEC is the vector released from the meshes after the trypsinization and removal of the first round (initially transduced) BAEC, these results unequivocally confirm

the transduction competence of Ad vectors released from the meshes during the 2-4 days interval after the commencement of virus release.

To confirm the findings of preserved transduction potential of chemically immobilized Ad vectors in the course of extended *in vitro* release, another sets of NHC-, SHC-, IHC- and RHC-tethered Ad-GFP meshes were exposed to complete cell growth medium (DMEM with 10% FBS) at 37°C with mild shaking for 3 days prior to extensive washing and relocation of the mesh disks into wells with freshly seeded BAEC. The ensuing GFP expression in cell cultures was monitored by fluorescent microscopy and fluorometry. Very low levels of GFP expression were observed in the wells treated with NHC- and SHC-containing meshes (Fig. 5c and d). However, the cells transduced using the pre-released meshes, employing IHC and RHC for vector immobilization, demonstrated significant transgene expression (Fig. 5c and d), which was only 2-fold lower than the transduction levels observed with the meshes used for cell transduction immediately upon preparation (compare Fig. 4d and 5d). Interestingly, the difference between transduction profiles of RHC- and IHC-containing meshes was less prominent in the cells transduced with pre-released meshes in comparison with the cells treated by the respective non-released counterparts (Fig. 4d and 5d). The latter finding is in agreement with a larger depletion of the meshes configured using RHC versus IHC vector linkage during the pre-plating adenoviral release phase.

Stent-based transduction of rat carotid arteries with Ad-Luc vectors immobilized to steel surface using HC with different kinetics of hydrolysis

To investigate whether modification of vector release and transduction profiles achieved *in vitro* using HC with dissimilar hydrolysis kinetics can be reproduced in vascular tissue of living animals, endovascular stents configured with 1.3×10^{10} Ad-Luc particles immobilized on the $PABT/PEI_{PDT}$ – treated stent surface through either NHC, SHC, IHC or RHC tethers were deployed in balloon-injured carotid arteries of Sprague-Dawley rats. Animals stented with BMS followed by local intralumenal delivery of 1.3×10^{10} Ad-Luc served as non-immobilized Ad vector control. Luciferase expression was studied in living animals by bioluminescence imaging following systemic administration of 50 mg luciferin. Signals emitted from the stented carotid arteries of rats implanted with the SHC-, IHC- and RHC-configured stents 1 day after stent deployments were respectively 146-, 273- and 496-fold higher than in the animals treated with stents employing a non-hydrolysable analog, sulfo-LC-SPDP, for vector tethering. The animals implanted with BMS and intralumenally delivered an equivalent dose (1.3×10^{10} viral particles) of free, non-modified Ad-Luc exhibited bioluminescence signal comparable with those achieved using vector tethering through RHC, IHC and SHC (Fig. 6a and b). The difference between vascular transgene expression in the RHC, IHC and SHC groups was not statistically significant, although the SHC-configured gene stents tended to result in a lower signal. The imaging was repeated 8 days after stent deployment. Arterial luciferase expression levels had dropped significantly in the animals treated with free vector and RHC modified gene eluting stents in comparison with transgene expression observed at 1 day post-stenting (2.5- and 1.8-fold, respectively; Fig. 6a and b). In contrast, increase of the average bioluminescence signal between days 1 and 8 was observed in animals treated with IHC and SHC-modified stents (1.4- and 1.8-fold, respectively; Fig. 6a and b).

DISCUSSION

Localized delivery of substrate-immobilized gene vectors has gained attention as a clinically translatable approach for the delivery of therapeutic transgenes in the setting of medical conditions that require implantation of temporary or permanent bioprosthetic devices, such as urological, bronchial and endovascular stents, orthopedic implants and pacemakers [38-41]. The added benefit of gene therapy provided in combination with medical device

implantation is two-fold: 1) to increase the therapeutic effectiveness of the implant and 2) to promote its integration into the host tissues. Endovascular stents [14], widely applied to treat atherosclerotic obstruction in coronary, carotid and peripheral circulation, are only partially effective since a significant fraction of patients develop a secondary “restenotic” obstruction of stented arteries due to uncontrolled activation of smooth muscle cells, leading to their proliferation, centripetal migration toward the arterial intima, and elaboration of abundant extracellular matrix encroaching on the lumen[16]. Therefore, augmenting the therapeutic effectiveness of stenting by combining the structural facilities of bare metal stents with stent-based gene therapy targeting the core mechanisms of restenosis came into sight as a logical extension of drug-eluting stent technology [17, 41].

Previous experimental work from our group [20, 22, 26, 27, 29], as well as from others [11, 19, 21, 24, 28, 30-32] has established the feasibility and therapeutic efficacy of gene vector immobilization on the surface of stents for the prevention of in-stent restenosis. However, methods previously used for tethering gene therapeutics to stent struts do not allow for strict control over the release rate of the vectors [20, 21, 26, 29, 42]. Numerous reports [43, 44] have documented that suppressed neointimal growth can recur if the inhibiting modality is withdrawn early, thus advocating for a sustained release of gene vectors over a 2-4 week vulnerability period. However, in the majority of published studies employing passive immobilization of gene vectors in a stent coating, up to 90% of vector payload is typically released within 24-48 hours [21, 42, 45]. Furthermore, bulk immobilization of viral and non-viral vectors in polymer coatings engineered on the surface of stents is associated with polymer-triggered inflammatory reaction [46]. To this end, our study demonstrates that immobilization of Ad vectors on PABT-modified, uncoated stainless steel results in a protracted (more than 1 month) time course of vector release. Moreover, the release rate of adenovectors from the substrate can be modulated to an extent by cross-linker chemistry and the concentration used for vector coupling. In our experiments vector tethered to solid support remains capable of transduction for 2-4 days after exposure to chemical environment and temperature conditions that cause rapid deterioration (1-2 log/day) of free adenovector [47]. This important finding suggests that stent tethering of gene vectors via HC can prolong the temporal window of stent-based gene delivery to affect both resident arterial cells and blood borne inflammatory cell types that typically get recruited to the angioplasty site within several days of stent placement [48].

A comparison of vector release kinetics and the respective transduction profiles of mesh-immobilized Ad vectors prepared using NHC, SHC, IHC and RHC demonstrated a correlation between the expected rate of ester bond hydrolysis in a HC backbone, vector release, and subsequent cell transduction *in vitro*. Indeed, at any time point, RHC-tethered Ad vector exhibited faster release from the steel substrate than IHC- and especially SHC-immobilized Ad vector. This dissimilarity in vector release rates translated into different peak levels of transgene expression and duration of the expression plateau attainable with the individual HC.

Since NHC does not contain any cleavable moieties, the virtually identical vector release kinetics from samples formulated using NHC and SHC vector tethering suggests that at the concentration used for Ad modification (500 μM), no identifiable ester hydrolysis-mediated release of vector occurs with SHC tethering in the time-frame of this experiment (Fig. 2a, 30 days). Nevertheless, in contrast to the NHC-tethered vector, SHC-tethered Ad-GFP possesses distinct transduction activity *in vitro* (Fig. 4a-d) and *in vivo* (Fig. 6a and b). It is feasible that the release of SHC-bound vector in amounts below the limit of detection is responsible for the localized transgene expression. Furthermore, a non-specific attachment of complex proteinaceous assemblies to the surface has been demonstrated to result in partial denaturation and the loss of functional properties of surface-bound material [49].

Moreover, exposing Ad vectors to catheters used for cardiovascular gene delivery was shown to result in a rapid deterioration of infective vector titers [50], presumably because of virus interaction with catheter material since pre-flushing of the catheters with albumin solution prevented virus titer loss [50]. Therefore, a non-specific attachment of Ad vectors to the PABT-modified steel surface may result in release of damaged Ad vector possessing minimal transduction activity. On the other hand, even very slow ester hydrolysis-mediated release of the vector attached via SHC tethering leads to effective transduction. This mechanistic difference alone can explain why seemingly identical vector release rates observed with SHC and NHC tethering may lead to vastly different transduction profiles (Fig. 4). Alternatively, the release of 20% of the initial virus load with NHC tethering can be explained by a reductive cleavage of disulfide bridges formed during vector tethering in the course of reaction between pyridyldithio groups of HC-modified Ad vector and thiol groups introduced onto steel surface. However, this scenario appears to be less probable since it does not reconcile release and transduction discrepancies observed with NHC and SHC tethering. Additionally, disulfide bonds are known to be relatively stable in a pro-oxidative extracellular microenvironment [51]. Transduction of arterial tissue with stent-tethered Ad-Luc resulted in site-specific transgene expression at the location of stent implantation. Although rat carotid luciferase expression 1 day after deployment of RHC stents was 1.8- and 3.4-fold higher than in arteries of rats receiving IHC and SHC stents, respectively, these differences were not statistically significant. Ad-Luc stent tethering via any of the three HC resulted in significantly higher ($p<0.05$) luciferase expression than was observed in animals treated with stents formulated using a non-hydrolysable cross-linker (NHC), sulfo-LC-SPDP, validating a key role of linker's shaft hydrolysis in productive *in vivo* transduction of arterial tissue.

An equivalent dose of free unmodified Ad-Luc vector dwelled in the stented segment of the artery for 20 min resulted in the levels of luciferase expression comparable to those observed using HC tethering of Ad-Luc to stents. This finding reflects remarkable augmentation of Ad transduction potency upon vector immobilization since 1) only a small fraction of stent-tethered vector is immediately mobilizable and thus able to contribute to arterial wall transduction at the day 1 time point (Fig. 2a and b) and 2) specific transduction effectiveness of HC-modified vectors is about 2 orders of magnitude lower than that of non-modified Ad (Fig. 4e).

A notable decrease of arterial transgene expression levels observed between days 1 and 8 post-procedure in the animals treated with free non-modified Ad-Luc and RHC-tethered Ad-Luc (Fig. 6a and b) reflects a common shortcoming of first generation Ad vectors as they lead to strong, but short-lived transgene expression due to the generation of an intensive inflammatory response against both virus and Ad-transduced cells [1]. To this end, vectors with a protracted expression profile *in vivo*, such as AAV, were recently demonstrated (data not shown) to lend themselves to immobilization onto steel surfaces via the same chemical modifications used in this study. In contrast with the decreasing luciferase expression in the carotid arteries of animals treated with RHC-configured stents, the bioluminescence signals emitted from the arteries treated with the IHC- and SHC-formulated stents demonstrated increased intensity at day 8 compared to the day 1 time point. A protracted release of transduction-competent Ad vectors beyond the initial release phase enabled by the deferred hydrolysis of IHC and SHC is the most plausible explanation of the dissimilar transduction kinetics in these groups of animals.

CONCLUSIONS

Our studies demonstrate that the use of a panel of hydrolysable cross-linker tethers with dissimilar $t_{1/2}$ of cross-linker cleavage can fine-tune the release rate of viral vectors from the

metal surface of medical implants, thus enabling modulation of the time course of ensuing localized transduction in the interfacing tissue.

Acknowledgments

The described studies were funded by a Scientist Development Grant from the American Heart Association to IF (0735110N) and NIH NHLBI to RJL (R01-72108). PTA catheters were kindly provided by NuMed (Hopkinton, NY). Authors wish to acknowledge secretarial assistance of Susan Kerns.

REFERENCES

[1]. Wu TL, Ertl HC. Immune barriers to successful gene therapy. Trends Mol Med. 2009; 15:32–9. [PubMed: 19101205]

[2]. Papadakis ED, Nicklin SA, Baker AH, White SJ. Promoters and control elements: designing expression cassettes for gene therapy. Curr Gene Ther. 2004; 4:89–113. [PubMed: 15032617]

[3]. Ladage D, Ishikawa K, Tilemann L, Muller-Ehmsen J, Kawase Y. Percutaneous methods of vector delivery in preclinical models. Gene Ther. 2012; 19:637–41. [PubMed: 22418064]

[4]. Bonadio J. Tissue engineering via local gene delivery. J Mol Med (Berl). 2000; 78:303–11. [PubMed: 11001527]

[5]. Zhao L, Wu J, Zhou H, Yuan A, Zhang X, Xu F, et al. Local gene delivery for cancer therapy. Curr Gene Ther. 2011; 11:423–32. [PubMed: 21711227]

[6]. Aoyama T, Yamamoto S, Kanematsu A, Ogawa O, Tabata Y. Local delivery of matrix metalloproteinase gene prevents the onset of renal sclerosis in streptozotocin-induced diabetic mice. Tissue Eng. 2003; 9:1289–99. [PubMed: 14674437]

[7]. Gruchala M, Roy H, Bhardwaj S, Yla-Herttuala S. Gene therapy for cardiovascular diseases. Curr Pharm Des. 2004; 10:407–23. [PubMed: 14965202]

[8]. Sharif F, Daly K, Crowley J, O'Brien T. Current status of catheter- and stent-based gene therapy. Cardiovasc Res. 2004; 64:208–16. [PubMed: 15485679]

[9]. Fishbein I, Stachelek SJ, Connolly JM, Wilensky RL, Alferiev I, Levy RJ. Site specific gene delivery in the cardiovascular system. J Control Release. 2005; 109:37–48. [PubMed: 16298010]

[10]. Ziauddin J, Sabatini DM. Microarrays of cells expressing defined cDNAs. Nature. 2001; 411:107–10. [PubMed: 11333987]

[11]. Jang JH, Koerber JT, Gujraty K, Bethi SR, Kane RS, Schaffer DV. Surface immobilization of hexa-histidine-tagged adeno-associated viral vectors for localized gene delivery. Gene Ther. 2010; 17:1384–9. [PubMed: 20508598]

[12]. Segura T, Shea LD. Surface-tethered DNA complexes for enhanced gene delivery. Bioconjug Chem. 2002; 13:621–9. [PubMed: 12009954]

[13]. Pannier AK, Shea LD. Controlled release systems for DNA delivery. Mol Ther. 2004; 10:19–26. [PubMed: 15233938]

[14]. Serruys PW, Kutryk MJ, Ong AT. Coronary-artery stents. N Engl J Med. 2006; 354:483–95. [PubMed: 16452560]

[15]. Roger VL, Go AS, Lloyd-Jones DM, Adams RJ, Berry JD, Brown TM, et al. Heart disease and stroke statistics--2011 update: a report from the American Heart Association. Circulation. 2011; 123:e18–e209. [PubMed: 21160056]

[16]. Sarkar K, Sharma SK, Sachdeva R, Romeo F, Garza L, Mehta JL. Coronary artery restenosis: vascular biology and emerging therapeutic strategies. Expert Rev Cardiovasc Ther. 2006; 4:543–56. [PubMed: 16918273]

[17]. Appleby CE, Kingston PA. Gene therapy for restenosis--what now, what next? Curr Gene Ther. 2004; 4:153–82. [PubMed: 15180583]

[18]. Kishore R, Losordo DW. Gene therapy for restenosis: Biological solution to a biological problem. J Mol Cell Cardiol. 2007; 42:461–8. [PubMed: 17222423]

[19]. Egashira K, Nakano K, Ohtani K, Funakoshi K, Zhao G, Ihara Y, et al. Local delivery of anti-monocyte chemoattractant protein-1 by gene-eluting stents attenuates in-stent stenosis in rabbits and monkeys. Arterioscler Thromb Vasc Biol. 2007; 27:2563–8. [PubMed: 17885211]

[20]. Klugherz BD, Jones PL, Cui X, Chen W, Meneveau NF, DeFelice S, et al. Gene delivery from a DNA controlled-release stent in porcine coronary arteries. Nat Biotechnol. 2000; 18:1181–4. [PubMed: 11062438]

[21]. Ohtani K, Egashira K, Nakano K, Zhao G, Funakoshi K, Ihara Y, et al. Stent-based local delivery of nuclear factor-kappaB decoy attenuates in-stent restenosis in hypercholesterolemic rabbits. Circulation. 2006; 114:2773–9. [PubMed: 17130346]

[22]. Perlstein I, Connolly JM, Cui X, Song C, Li Q, Jones PL, et al. DNA delivery from an intravascular stent with a denatured collagen-polylactic-polyglycolic acid-controlled release coating: mechanisms of enhanced transfection. Gene Ther. 2003; 10:1420–8. [PubMed: 12900756]

[23]. Takemoto Y, Kawata H, Soeda T, Imagawa K, Somekawa S, Takeda Y, et al. Human placental ectonucleoside triphosphate diphosphohydrolase gene transfer via gelatin-coated stents prevents in-stent thrombosis. Arterioscler Thromb Vasc Biol. 2009; 29:857–62. [PubMed: 19325141]

[24]. Walter DH, Cejna M, Diaz-Sandoval L, Willis S, Kirkwood L, Stratford PW, et al. Local gene transfer of phVEGF-2 plasmid by gene-eluting stents: an alternative strategy for inhibition of restenosis. Circulation. 2004; 110:36–45. [PubMed: 15210598]

[25]. Zhang LH, Luo T, Zhang C, Luo P, Jin X, Song CX, et al. Anti-DNA antibody modified coronary stent for plasmid gene delivery: results obtained from a porcine coronary stent model. J Gene Med. 2011; 13:37–45. [PubMed: 21259407]

[26]. Fishbein I, Alferiev I, Nyanguile O, Gaster R, Vohs JM, Wong GS, et al. Bisphosphonate-mediated gene vector delivery from the metal surfaces of stents. Proc Natl Acad Sci U S A. 2006; 103:159–64. [PubMed: 16371477]

[27]. Fishbein I, Alferiev I, Bakay M, Stachelek SJ, Sobolewski P, Lai M, et al. Local delivery of gene vectors from bare-metal stents by use of a biodegradable synthetic complex inhibits in-stent restenosis in rat carotid arteries. Circulation. 2008; 117:2096–103. [PubMed: 18413497]

[28]. Johnson TW, Wu YX, Herdeg C, Baumbach A, Newby AC, Karsch KR, et al. Stent-Based Delivery of Tissue Inhibitor of Metalloproteinase-3 Adenovirus Inhibits Neointimal Formation in Porcine Coronary Arteries. Arterioscler Thromb Vasc Biol. 2005; 25:754–9. [PubMed: 15681295]

[29]. Klugherz BD, Song C, DeFelice S, Cui X, Lu Z, Connolly J, et al. Gene delivery to pig coronary arteries from stents carrying antibody-tethered adenovirus. Hum Gene Ther. 2002; 13:443–54. [PubMed: 11860711]

[30]. Sharif F, Hynes SO, McMahon J, Cooney R, Conroy S, Dockery P, et al. Gene-eluting stents: comparison of adenoviral and adeno-associated viral gene delivery to the blood vessel wall in vivo. Hum Gene Ther. 2006; 17:741–50. [PubMed: 16839273]

[31]. Sharif F, Hynes SO, Cooney R, Howard L, McMahon J, Daly K, et al. Gene-eluting stents: adenovirus-mediated delivery of eNOS to the blood vessel wall accelerates re-endothelialization and inhibits restenosis. Mol Ther. 2008; 16:1674–80. [PubMed: 18714308]

[32]. Sharif F, Hynes SO, McCullagh KJ, Ganley S, Greiser U, McHugh P, et al. Gene-eluting stents: non-viral, liposome-based gene delivery of eNOS to the blood vessel wall in vivo results in enhanced endothelialization but does not reduce restenosis in a hypercholesterolemic model. Gene Ther. 2012; 19:321–8. [PubMed: 21716298]

[33]. O'Riordan CR, Lachapelle A, Delgado C, Parkes V, Wadsworth SC, Smith AE, et al. PEGylation of adenovirus with retention of infectivity and protection from neutralizing antibody in vitro and in vivo. Hum Gene Ther. 1999; 10:1349–58. [PubMed: 10365665]

[34]. Chorny M, Fishbein I, Yellen BB, Alferiev IS, Bakay M, Ganta S, et al. Targeting stents with local delivery of paclitaxel-loaded magnetic nanoparticles using uniform fields. Proc Natl Acad Sci U S A. 2010; 107:8346–51. [PubMed: 20404175]

[35]. Polyak B, Fishbein I, Chorny M, Alferiev I, Williams D, Yellen B, et al. High field gradient targeting of magnetic nanoparticle-loaded endothelial cells to the surfaces of steel stents. Proc Natl Acad Sci U S A. 2008; 105:698–703. [PubMed: 18182491]

[36]. Leopold PL, Ferris B, Grinberg I, Worgall S, Hackett NR, Crystal RG. Fluorescent virions: dynamic tracking of the pathway of adenoviral gene transfer vectors in living cells. Hum Gene Ther. 1998; 9:367–78. [PubMed: 9508054]

[37]. Bar T, Kubista M, Tichopad A. Validation of kinetics similarity in qPCR. Nucleic Acids Res. 2012; 40:1395–406. [PubMed: 22013160]

[38]. de Poorter JJ, Tolboom TC, Rabelink MJ, Pieterman E, Hoeben RC, Nelissen RG, et al. Towards gene therapy in prosthesis loosening: efficient killing of interface cells by gene-directed enzyme prodrug therapy with nitroreductase and the prodrug CB1954. J Gene Med. 2005; 7:1421–8. [PubMed: 15977303]

[39]. Guan Y, Ou L, Hu G, Wang H, Xu Y, Chen J, et al. Tissue engineering of urethra using human vascular endothelial growth factor gene-modified bladder urothelial cells. Artif Organs. 2008; 32:91–9. [PubMed: 18005271]

[40]. Rosen MR, Robinson RB, Brink PR, Cohen IS. The road to biological pacing. Nat Rev Cardiol. 2011; 8:656–66. [PubMed: 21844918]

[41]. Takahashi H, Letourneur D, Grainger DW. Delivery of large biopharmaceuticals from cardiovascular stents: a review. Biomacromolecules. 2007; 8:3281–93. [PubMed: 17929968]

[42]. Jewell CM, Zhang J, Fredin NJ, Wolff MR, Hacker TA, Lynn DM. Release of plasmid DNA from intravascular stents coated with ultrathin multilayered polyelectrolyte films. Biomacromolecules. 2006; 7:2483–91. [PubMed: 16961308]

[43]. Carter AJ, Aggarwal M, Kopia GA, Tio F, Tsao PS, Kolata R, et al. Long-term effects of polymer-based, slow-release, sirolimus-eluting stents in a porcine coronary model. Cardiovasc Res. 2004; 63:617–24. [PubMed: 15306217]

[44]. Sirois MG, Simons M, Kuter DJ, Rosenberg RD, Edelman ER. Rat arterial wall retains myointimal hyperplastic potential long after arterial injury. Circulation. 1997; 96:1291–8. [PubMed: 9286961]

[45]. Takahashi A, Palmer-Opolski M, Smith RC, Walsh K. Transgene delivery of plasmid DNA to smooth muscle cells and macrophages from a biostable polymer-coated stent. Gene Ther. 2003; 10:1471–8. [PubMed: 12900762]

[46]. van der Giessen WJ, Lincoff AM, Schwartz RS, van Beusekom HM, Serruys PW, Holmes DR Jr. et al. Marked inflammatory sequelae to implantation of biodegradable and nonbiodegradable polymers in porcine coronary arteries. Circulation. 1996; 94:1690–7. [PubMed: 8840862]

[47]. Croyle MA, Yu QC, Wilson JM. Development of a rapid method for the PEGylation of adenoviruses with enhanced transduction and improved stability under harsh storage conditions. Hum Gene Ther. 2000; 11:1713–22. [PubMed: 10954905]

[48]. Welt FG, Rogers C. Inflammation and restenosis in the stent era. Arterioscler Thromb Vasc Biol. 2002; 22:1769–76. [PubMed: 12426203]

[49]. Roach P, Farrar D, Perry CC. Interpretation of protein adsorption: surface-induced conformational changes. J Am Chem Soc. 2005; 127:8168–73. [PubMed: 15926845]

[50]. Marshall DJ, Palasis M, Lepore JJ, Leiden JM. Biocompatibility of cardiovascular gene delivery catheters with adenovirus vectors: an important determinant of the efficiency of cardiovascular gene transfer. Mol Ther. 2000; 1:423–9. [PubMed: 10933963]

[51]. Saito G, Swanson JA, Lee KD. Drug delivery strategy utilizing conjugation via reversible disulfide linkages: role and site of cellular reducing activities. Adv Drug Deliv Rev. 2003; 55:199–215. [PubMed: 12564977]

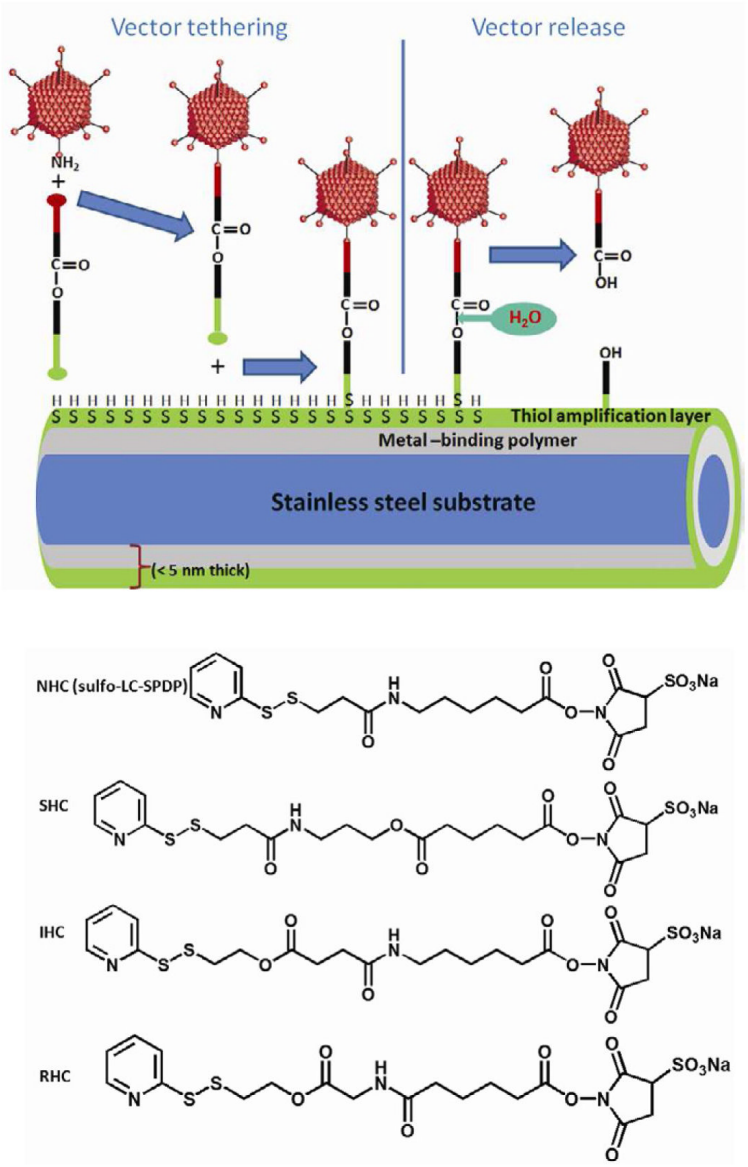

Figure 1. Chemical modification of Ad vector with HC for metal substrate attachment and hydrolysis-mediated release

A scheme representing Ad vector tethering to a PABT/PEI_{PDT}-modified stainless steel surface via a HC and subsequent release of the vector upon cross-linker hydrolysis is shown (A). See text for additional explanations. Structural formulas of cross-linkers (NHC, SHC, IHC and RHC) used throughout the described studies (B).

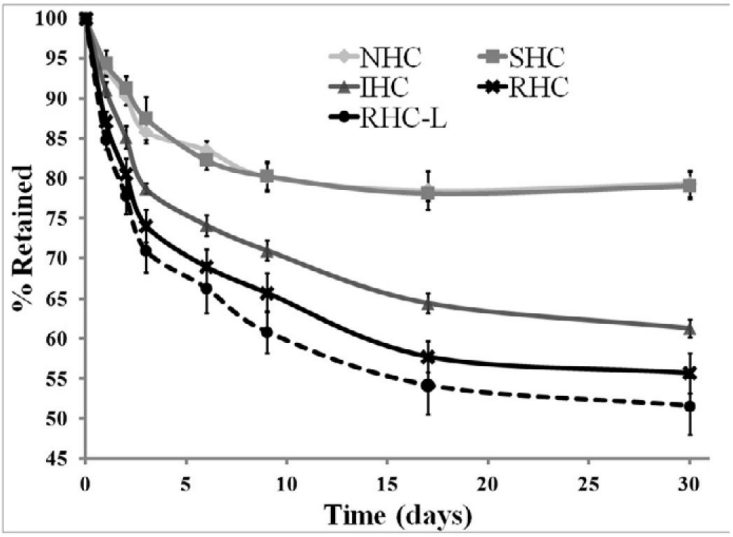

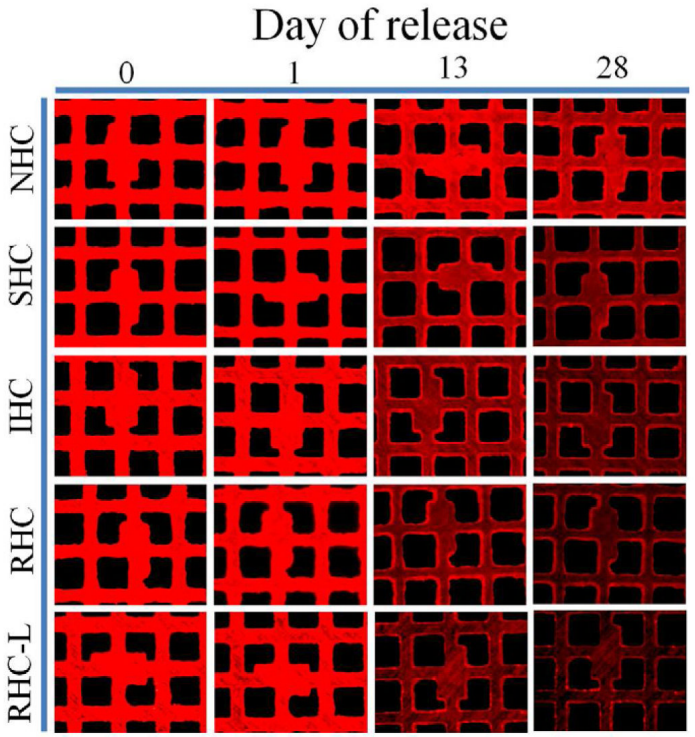

Figure 2. Release kinetics of Ad vector tethered to metal substrates with HC

316 grade stainless steel meshes were formulated with ~2×10^9 Cy3-labeled Ad particles attached to the PABT/PEI_{PDT}-modified surface after modification with 500 μM NHC, SHC, IHC, RHC and 100 μM RHC (designated as RHC-L). The release of fluorescently labeled Ad-particles was studied at the indicated time points by (A) well-scan fluorometry at 530/555 nm and (B) fluorescent microscopy (rhodamine filter set; original magnification 100×). Fluorometry results are presented as means ± SEM, n =8-10. $p<0.001$ for all comparisons between the NHC and SHC vs IHC, RHC and RHC-L groups were determined by Anova with a post-hoc Tukey test.

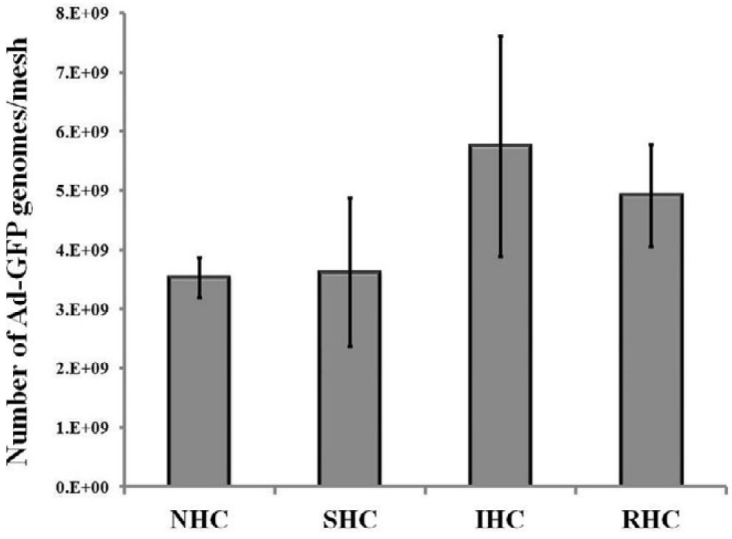

Figure 3. Amount of surface-immobilized Ad vector particles as determined by qPCR

The stainless steel meshes were configured with Ad-GFP immobilized via RHC, IHC, SHC or NHC (n=3 for each condition). After proteinase K treatment, viral DNA was eluted and purified using a QIAamp mini kit (Qiagen). Amplification of viral DNA using GFP-specific primers was carried out in SDS-7500 engine (Applied Biosystems) and detected with Sybr Green. Data normalization was based on a calibration curve prepared with a known amount of non-immobilized Ad-GFP.

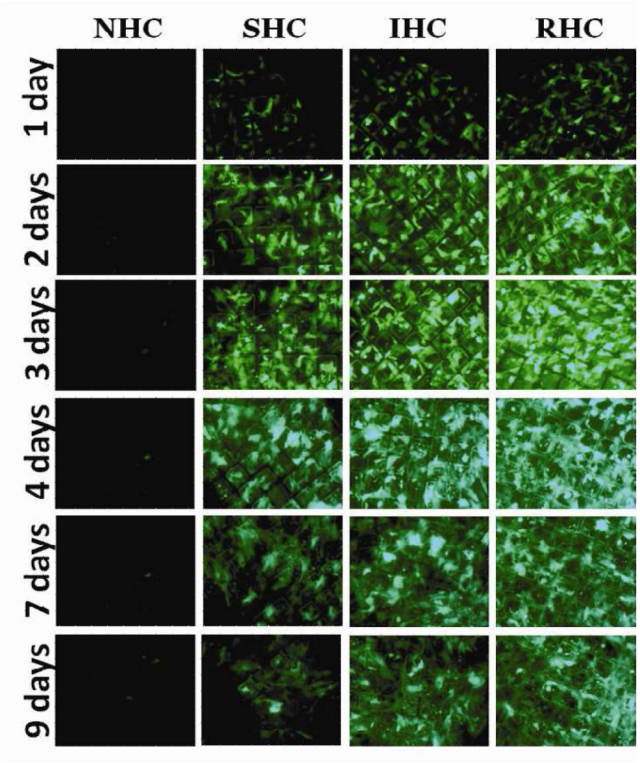

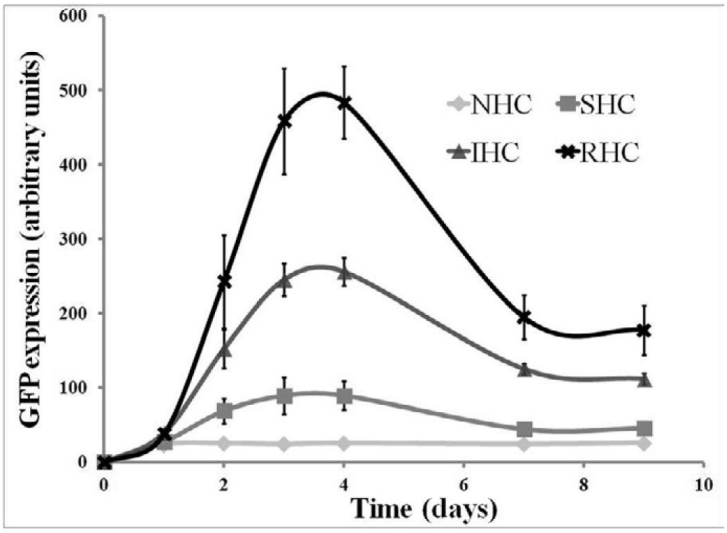

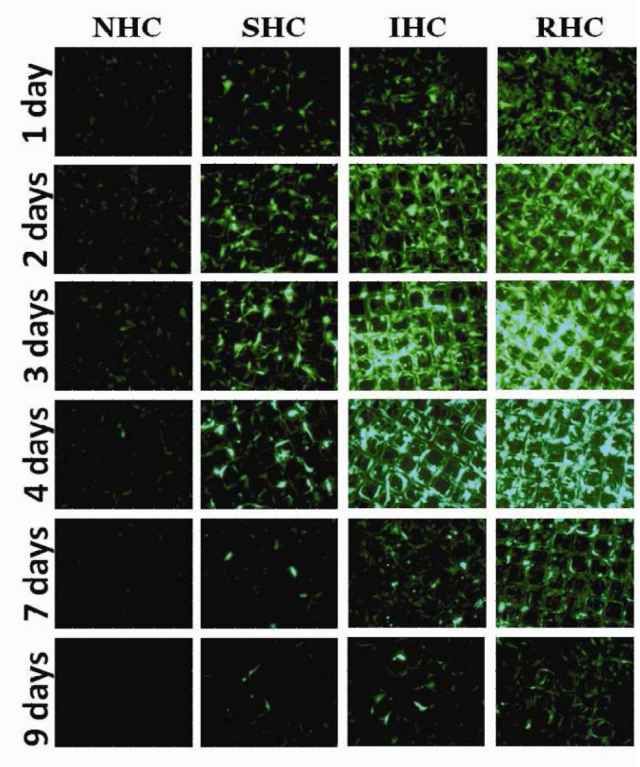

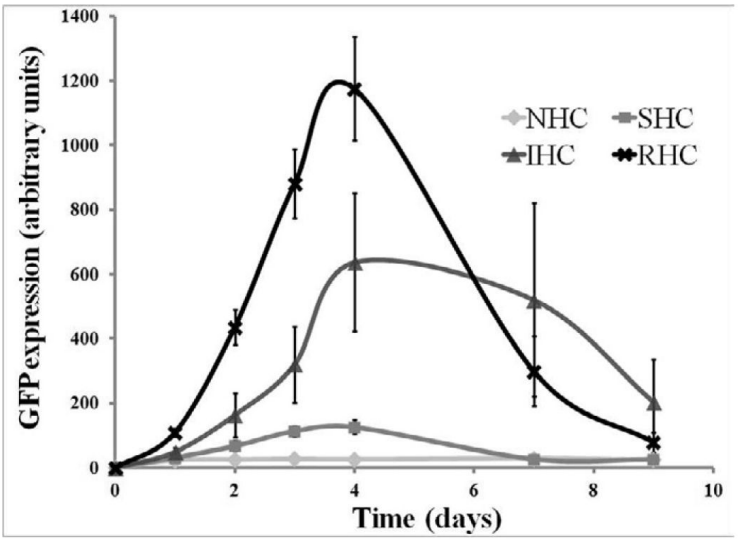

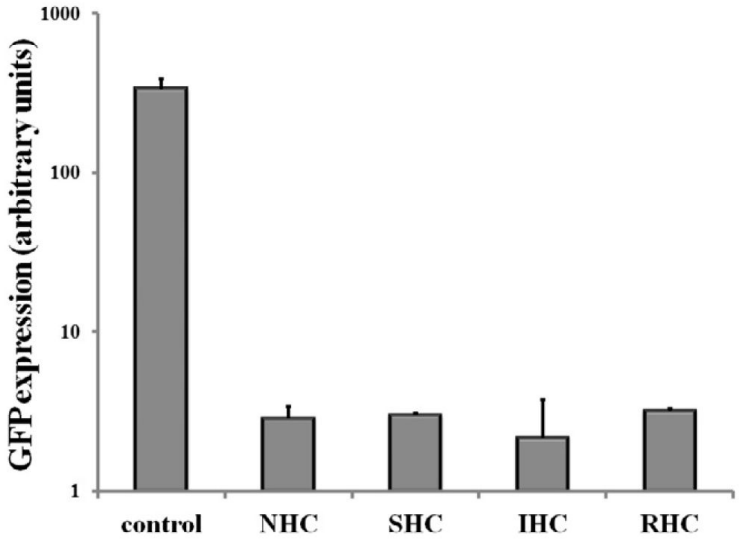

Figure 4. Transduction of BAEC and SMC with Ad vector immobilized to metal surfaces with HC

Meshes were derivatized with ~2×10^9 Ad-GFP particles appended via NHC, SHC, IHC and RHC. Meshes were then individually placed on top of confluent A10 (A, B) and BAEC (C, D) monolayers. Transduction (expressed as GFP expression levels) from cells treated with Ad vector-tethered meshes was assessed by fluorescence microscopy (A, C) and well-scan fluorometry (B, D). Fluorometry results are presented as means ± SEM, n =4 . Transduction of BAEC with non-immobilized Ad-GFP following modification with NHC, SHC, IHC and RHC (500 μM final concentration for all 4 cross-linkers) as compared to non-modified Ad-GFP (E). Fluorometry results are presented as means ± SEM, n =3.

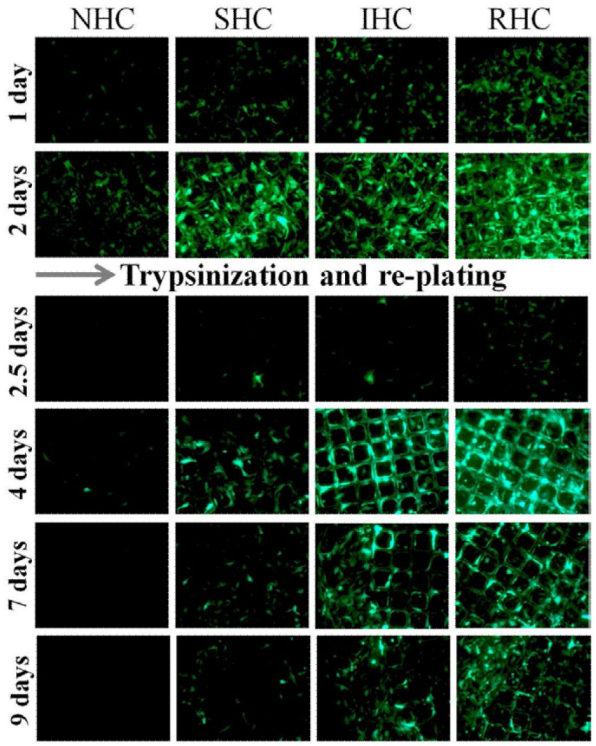

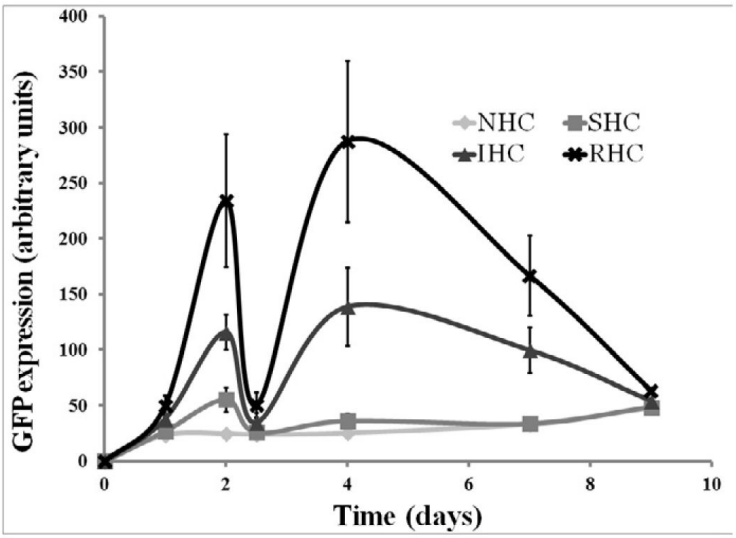

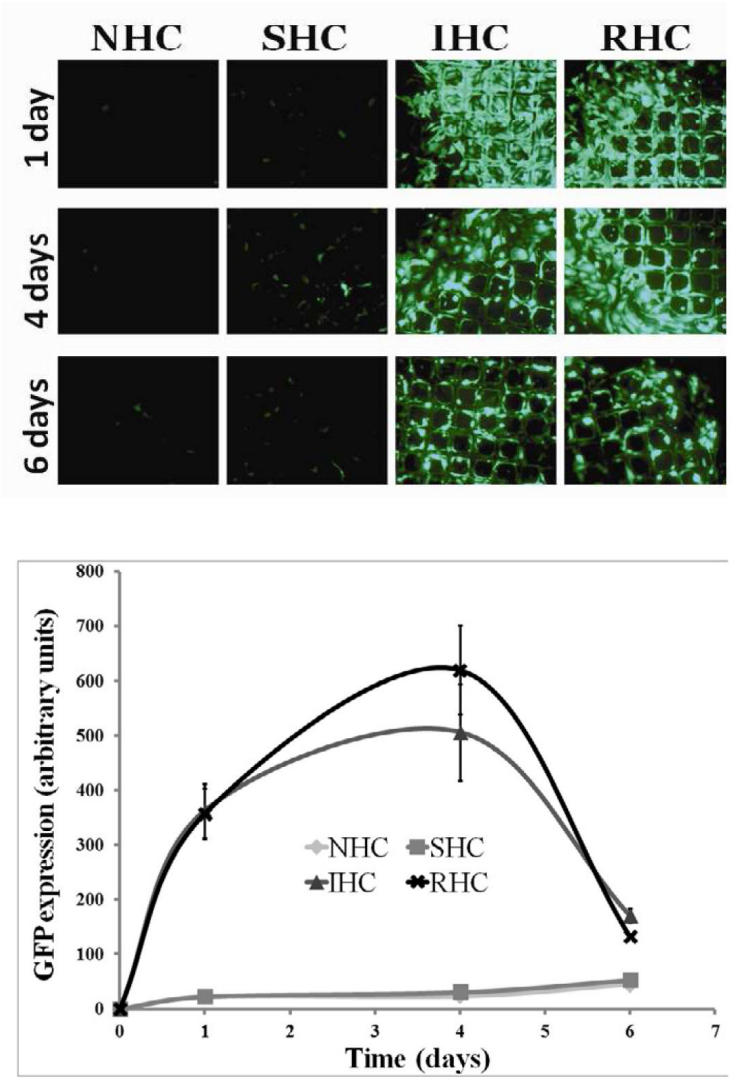

Figure 5. Transduction competence of substrate immobilized Ad vectors at delayed time points

Ad-GFP was tethered to metal meshes via NHC, SHC, IHC or RHC and the meshes were placed on a confluent monolayer of BAEC. Two days post mesh placements, BAEC were trypsinized and removed without disturbing the meshes. New, non-transduced cultures of BAEC were then seeded onto the meshes. Ad-GFP transduction competency was measured by GFP expression through fluorescent microscopy (A) and fluorometry (B). Measurements were taken at indicated days, representative images were used and fluorometry results are means ± SEM, $n = 4$ Another set of Ad-GFP tethered meshes were incubated in complete cell growth medium at 37°C with mild shaking for 3 days prior to placements on a confluent monolayer of BAEC. Ad-GFP transduction competency was measured by GFP expression through fluorescent microscopy (C) and fluorometry (D). Measurements were taken at indicated days, representative images were used and fluorometry results are presented as means ± SEM, $n = 4$.

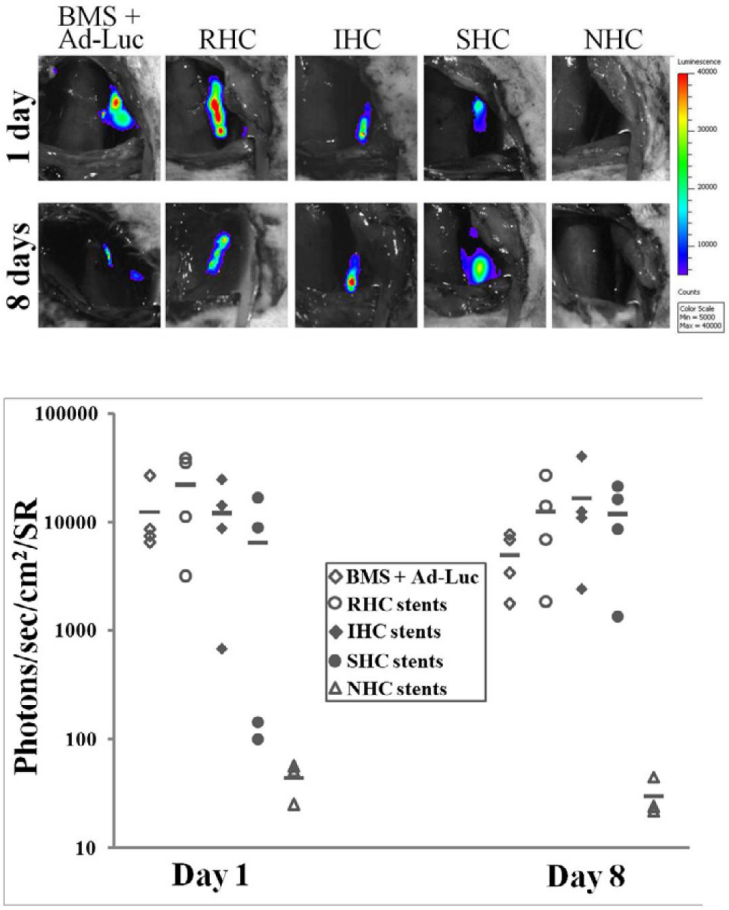

Figure 6. Transduction efficiency of Ad-Luc immobilized to metal surfaces with HC of differing kinetics of hydrolysis *in vivo*

Ad-Luc (1.3×10^{10} particles) was tethered to endovascular stents via NHC (n=3), SHC (n=4), IHC (n=4) or RHC (n=4) as described in the Materials and Methods. An additional group of animals (n=4) was implanted with BMS, and the stented segment was intralumenally instilled with 1.3×10^{10} Ad-Luc for 20 min. Transduction efficiency of Ad-Luc was measured by bioluminescence imaging (IVIS Spectrum) 1 and 8 days post stent deployment (A, B). Representative images were used. Individual data were plotted using a logarithmic scale. The respective means were presented as horizontal bars.